Occurrence, gas–particle partitioning, and sources of polybrominated diphenyl ethers in the atmosphere over the Yangtze River Estuary, East China Sea

Tianfeng Guo [a,b], Tian Lin [c], Yuanyuan Li [a], Zilan Wu [a], Yuqing Jiang [a], Zhigang Guo [a,b,*]

[a] Shanghai Key Laboratory of Atmospheric Particle Pollution and Prevention, Department of Environmental Science and Engineering, Fudan University, Shanghai 200433, China
[b] Shanghai Institute of Eco-Chongming (SIEC), Shanghai 200062, China
[c] State Key Laboratory of Environmental Geochemistry, Institute of Geochemistry, Chinese Academy of Sciences, Guiyang 550081, China

HIGHLIGHTS

- BDE-209 was dominated in total PBDEs in both gas and particle phases over the YRE.
- A strongly seasonal variation of the occurrence and gas-particle partitioning of PBDEs was observed.
- Gas-particle partitioning of PBDEs was in the non-equilibrium state, particularly prominent for BDE-209.
- BDE-209 over the YRE was influenced by atmospheric transport from land emissions in both phases.

GRAPHICAL ABSTRACT
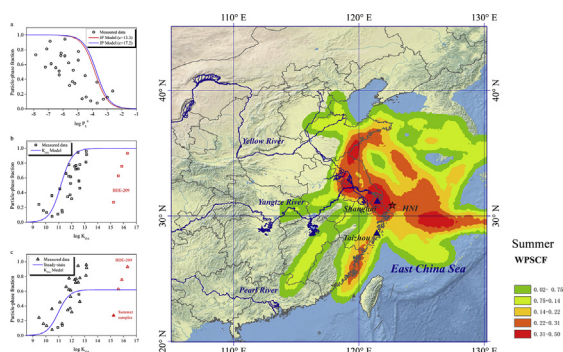
ARTICLE INFO

ABSTRACT

To investigate the occurrence, gas–particle partitioning, and potential sources of polybrominated diphenyl ethers (PBDEs) in the atmosphere over the Yangtze River Estuary, gas and particle samples were collected at the remote Huaniao Island, East China Sea, during a whole year from 2013 to 2014. Nine PBDEs, with total atmospheric concentration of Σ_9BDEs of 20.3 ± 26.5 pg/m^3, were found in both the gas and particle phases in most samples. BDE-209 dominated both the gas and particle phases, which is consistent with the PBDE usage record in China. Seasonal variation of particle-phase Σ_9BDEs was observed, with the highest concentration in winter and the lowest in summer; however, a reversed seasonal trend was observed in the gas phase. Correlation analysis between log K_p and log K_{OA} suggested that the gas–particle (G/P) partitioning was in a non-equilibrium state, particularly for BDE-209 throughout the year. The K_{OA}-based adsorption model prediction performed relatively well for the particle-phase fraction of Br$_{<10}$-BDEs, but largely overestimated BDE-209. A steady-state model could be superior to predict G/P partitioning of BDE-209 based on annual values, though with the exception of summer samples. A relatively higher gas-phase distribution for BDE-209 than high-brominated BDEs was observed, especially in summer, when it reached 73%, implying a sustained input of gas-phase BDE-209. The potential source

* Corresponding author at: Shanghai Key Laboratory of Atmospheric Particle Pollution and Prevention, Department of Environmental Science and Engineering, Fudan University, Shanghai 200433, China.
E-mail address: guozgg@fudan.edu.cn (Z. Guo).

contribution function showed that the possible source regions for BDE-209 included Shandong and Jiangsu Provinces (the main BDE-209 production regions in China), the Yangtze River Delta region, and the southeastern coastal areas (which hosts intensive electronic waste recycling activities).

1. Introduction

Polybrominated diphenyl ethers (PBDEs), organic compounds containing as many as ten bromine atoms, have been used as additive flame retardants since the 1970s in a wide range of consumer products and articles (Bergman et al., 2012). PBDEs are commercially produced in three forms: penta-BDE (composed of ~33% BDE-47, ~47% BDE-99, and ~8% BDE-100), octa-BDE (~25% BDE-183, ~31% BDE-197, and ~24% BDE-207), and deca-BDE (~93% BDE-209) (Darnerud et al., 2001). Due to their bioaccumulation potential, toxicity, persistence, and potential for atmospheric transport over long distances, the manufacture and use of PBDEs have been strictly regulated and partially prohibited in recent years. For example, components of the penta- and octa-BDE mixtures were included in the Stockholm Convention on Persistent Organic Pollutants (POPs) in 2009 (www.pops.int). In China, commercial mixtures of penta-BDE were banned from production in 2004, and octa-BDEs were never produced. However, China remains the largest producer and supplier of deca-BDE mixtures (Ni et al., 2013).

The manufacture, use, and disposal of items containing PBDEs are the major sources of PBDE emissions into the ambient environment. Primary sources of PBDEs include manufacturing sites, waste-related facilities, and wastewater treatment plants (Ma et al., 2012). In China, domestic deca-BDE manufacturing facilities are primarily located in Laizhou Bay, Shandong Province, as well as in Jiangsu Province (Ma et al., 2012; Yu et al., 2016). In addition, there are a considerable number of electronic waste (e-waste) recycling regions, especially in southern and southeastern China, i.e., Taizhou (Zhejiang Province), Guiyu (Guangdong Province), and Qingyuan (Guangdong Province) (Bi et al., 2007; Tian et al., 2011; Xu et al., 2015a, 2015b). Aside from these point sources, urban regions with high industries and dense population densities are also regarded as significant atmospheric sources. Due to the widespread distribution and application of daily-use products in above urban regions, PBDEs can be released by volatilization (Li et al., 2016a, 2016b).

Series of field observations for PBDEs have been conducted over various regions worldwide (Wang et al., 2010; Li et al., 2016a, 2016b; Liu et al., 2016; Yu et al., 2016; Ji et al., 2017). The sampling site of this study, Huaniao Island (HNI), is located in the Yangtze River Estuary (YRE) on the coast of the East China Sea (ECS), adjacent to the Yangtze River Delta (YRD) (Fig. 1), the most urbanized and industrialized region
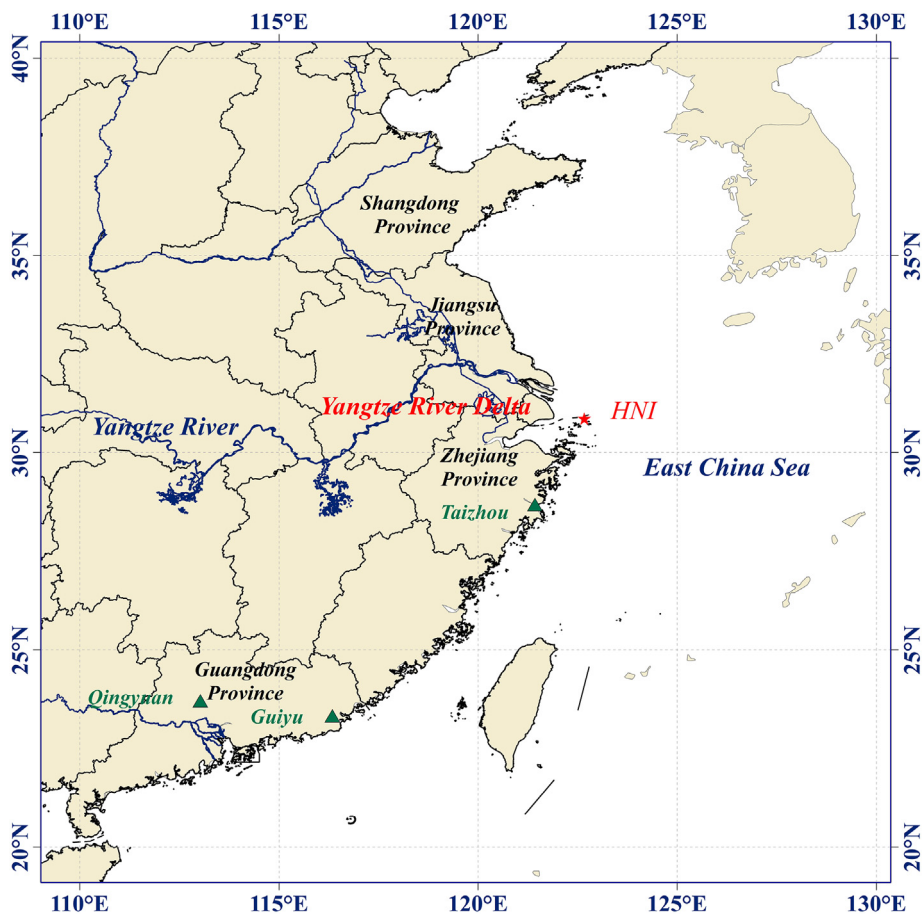

Fig. 1. Map of the sampling site. The red site is the sampling site (Huaniao Island), the green triangles represent e-waste recycling sites in China. (For interpretation of the references to colour in this figure legend, the reader is referred to the web version of this article.)

in China. The site is downwind of the YRD region and is largely influenced by the East Asian Monsoon. Due to its rapid industrialization and urbanization, the YRD, which covers only 1.1% of the area of China, is home to 108 million people (8.1% of the total population of China) (Wang et al., 2015); in 2011, it represented 17.4% of the entire Chinese economy (www.hktdc.com). The atmosphere at HNI could be influenced by both ambient emissions and long-range transport. Because there is almost no industrial activity, the site is ideal for monitoring background/rural pollution and the transport of pollutants such as polycyclic aromatic hydrocarbons (Jiang et al., 2018) and organochlorine pesticides (Li et al., 2017). Li et al. (2015a) reported the seasonal variation of PBDEs in fine particulate matter ($PM_{2.5}$) over the YRE. PBDEs in gas and particle phases differ in terms of concentration, seasonal variation, and removal from the atmosphere. In addition, the gas–particle (G/P) partitioning of PBDEs over the estuary remains poorly explored.

In this study, 95 pairs of total suspended particulate and polyurethane foam (PUF) atmospheric samples were collected at Huaniao Island, YRE, from October 2013 to July 2014 and analyzed for PBDEs. The objectives of this study were to (1) determine the concentration and seasonal variation of PBDEs in the atmosphere over the YRE, (2) calculate the phase distribution and gas–particle partitioning of PBDEs over the YRE, and (3) identify the potential sources of the dominant congener BDE-209 based on the potential source contribution function.

2. Materials and methods

2.1. Sampling

Sampling was performed as described previously (Li et al., 2017; Jiang et al., 2018). In brief, the gas and aerosol samples were collected from October 2013 to August 2014 at HNI (30.86°N, 122.67°E) in the YRE, ECS. Approximately 66 km off the coast of mainland China, HNI is a small rural island in the ECS. It has a population of <1000 and has no local industrial activity. Gas- and aerosol-phase samples were collected simultaneously using a high-volume air sampler (300 L/min; Guangzhou Mingye Technology Company, Guangzhou, China), which was deployed on the roof of a three-story building at the northernmost point of HNI (50 m above sea level) for about 24 h. Particle-phase PBDEs were trapped using a pre-combusted quartz filter (20 × 25 cm, 2600QAT; Pall Gelman, Port Washington, NY, USA), while gas-phase PBDEs were collected using a solvent-cleaned PUF plug (8.0 cm length, 6.25 cm diameter, 0.035 g/cm³ density). In total, 95 pairs of air and aerosol samples were collected. Two field blank samples were employed for each season to assess potential contamination during sampling. Breakthrough of the PUF samples was tested using two consecutive PUF plugs. All samples were stored at −20 °C until further analysis.

2.2. Chemical analysis

Sample extraction, clean-up, and analysis were performed using the methods described in our previous work (Li et al., 2015a, 2015b; Jiang et al., 2018). Briefly, the samples were Soxhlet-extracted for 48 h using dichloromethane (DCM) after spiking with known amounts of a mixture of ^{13}C-labled PBDE standards (BDE-28, 47, 99, 100, 153, 154, 183, and 209; Cambridge Isotope Laboratories, Andover, MA, USA) as surrogates. Then, the extracts were concentrated using a rotary evaporator and solvent-exchanged with n-hexane. The concentrated extracts were then purified using a mixed-layer chromatography column (8 mm diameter), consisting of 3 cm deactivated alumina, 3 cm deactivated silica gel, and 1 cm anhydrous sodium sulfate (from bottom to top), and eluted with 50 mL of a mixture of DCM and hexane (1:1 by volume). Finally, the extracts were concentrated to 0.5 mL, and then spiked with a known quantity of BDE-77 as an internal standard prior to instrumental analysis. PBDEs were analyzed by gas chromatography–

mass spectrometry (GC–MS; GC7890 coupled with 5975C MSD; Agilent, Santa Clara, CA, USA), using negative chemical ionization (NCI) in selected ion monitoring (SIM) mode. Chromatographic separation was achieved using a DB-5MS capillary column (9 m × 0.25 mm × 0.1 μm) and a longer column (30 m × 0.25 mm × 0.25 μm) for BDE-209 and $Br_{<10}$-PBDE congeners, respectively.

2.3. Quality assurance and quality control

Strict procedures were implemented during the sampling and processing stages. Field blanks, laboratory blanks (solvent), and spiked blanks (nine standard PBDE congeners spiked into the solvent) were analyzed in the same manner as the samples. Samples containing PBDE concentrations below the method detection limit (MDL; 0.04 pg/m³ for BDE-209 and 0.01 pg/m³ for other individual PBDE congeners) were considered as not detected. The field and laboratory blank samples contained target compound concentrations lower than their MDLs. Breakthrough testing of the PUF samples using two consecutive PUF plugs showed that the target compound concentrations in the second PUF plug were lower than their MDLs.

For each batch of ten samples, a spiked blank was processed for quality assurance and control. The average standard recovery for the spiked blanks was 88.0 ± 8.5%. Though a mixture ^{13}C-labeled PBDE standards was spiked, only ^{13}C-labeled BDE-47 and ^{13}C-labeled BDE-209 were calculated to indicate their recovery for $Br_{<10}$-BDEs and BDE-209, respectively. The recovery of ^{13}C-labeled BDE-47 for $Br_{<10}$-BDEs was in the range of 55.6–89.3% (72 ± 25%); the value of ^{13}C-labeled BDE-209 for BDE-209 was in the range of 48.5–98.2% (76 ± 30%). The concentration of $Br_{<10}$-BDEs and BDE-209 in each sample were corrected based on the corresponding surrogate recovery of the distinct sample.

2.4. Gas–particle partitioning

Partitioning of atmospheric semi-volatile organic compounds (SVOCs) between the gas and particle phases was defined by the particle–gas partition coefficient, K_p (m³/μg):

$$K_p = \frac{C_p / TSP}{C_g} \tag{1}$$

where C_p and C_g are the SVOC concentrations in the gas and particle phases (pg/m³ of air), respectively, and TSP is the concentration of total suspended particulate matter in air (μg/m³).

According to Pankow (1994), PBDE gas–particle partitioning can be driven by two mechanisms: adsorption onto the particle surface and absorption into particle organic matter. These two mechanisms can both lead to a similar linear relationship between log K_p and the logarithm of the subcooled liquid vapor pressure (P_L^0, Pa) of the compound, which can be expressed as follows:

$$\log K_p = m_p \times \log P_L^0 + b_p \tag{2}$$

where slope m_p and intercept b_p are fitting constants obtained using the regression of log K_p against log P_L^0.

The values of P_L^0 are temperature dependent and can be calculated using the following equation (Tittlemier et al., 2002):

$$\log P_L^0 = A_p + B_p/T \tag{3}$$

The octanol–air partition coefficient (K_{OA})-based absorption model is usually used to predict the values of K_p and is a better descriptor of gas–particle partitioning (Finizio et al., 1997). The relationship between log K_p and log K_{OA} can be described as follows:

$$\log K_p = m_o \times \log K_{OA} + b_o \tag{4}$$

where slope m_0 and intercept b_0 are fitting constants obtained using the regression of $\log K_P$ against $\log K_{OA}$. K_{OA} is given by an empirical equation (Harner and Shoeib, 2002; Li et al., 2016a, 2016b):

$$\log K_{OA} = A_0 + B_0/T \tag{5}$$

In addition, a steady-state model recently suggested by Li et al. (2015b) was also occupied in this study (details in Supplementary Material Text S1), which has been proved to be a better predictor for gas–particle partitioning of BDE-209 (Besis et al., 2017).

2.5. Potential source contribution function

Air mass back-trajectories were calculated starting at 20:00 local standard time for 48 h at a height of 500 m above ground level by running the NOAA Air Resource Lab HYSPLIT model (http://www.arl.noagov/ready/hysplit4.html). The potential source contribution function (PSCF) (Ashbaugh et al., 1985; Hsu et al., 2003; Wang et al., 2016) was calculated to infer the potential source regions that caused elevated concentrations of PBDEs at the receptor site. The particle-phase BDE-209 concentrations of each sample were used as input data for the PSCF analysis. The detailed calculation method is described in the Supplementary Material (Text S2).

3. Results and discussion

3.1. Occurrence

Nine PBDEs (BDE-28, −47, −99, −100, −153, −154, −138, −183, and −209) were detected in both the gas and particle phases in most atmospheric samples (> 90%), with a mean total atmospheric concentration (particle phase plus gas phase) Σ_9BDEs of 20.3 ± 26.5 m³. As reported by Yang et al. (2013), total atmospheric concentrations of $\sum_{12}$BDEs in China followed as the order urban (306 ± 20.0 pg/m³) > suburban (67.0 ± 14.0 pg/m³) > background/rural (14.0 ± 1.0 pg/m³). Additionally, around the Great Lakes in the United States, total atmospheric $\sum_{12}$BDEs concentrations were highest at two urban sites (65 ± 4 and 87 ± 8 pg/m³, respectively) and lowest at a remote site (5.8 ± 0.4 pg/m³) (Venier and Hites, 2008). Atmospheric PBDE concentrations over the global oceans, influenced by the distance to possible source regions, emissions, environmental parameters, as well as temperature-related effects, have generally been recorded in the hundreds of femtograms to the picograms per cubic meter range (Möller et al., 2011a, 2012b). For examples, total atmospheric concentrations ($\sum_{10}$BDEs) ranged from 0.07 to 8.1 pg/m³ during a cruise from East Asia to the Pacific Ocean and then further to the Arctic (Möller et al., 2011a) and from undetected to 6.6 pg/m³ from the East Indian

Table 1

Atmospheric PBDE levels from studies reported worldwide (unit: pg/m³). The * indicted concentration with ng/m³ unit.

| Area	Date	Congeners	Device	Phase	BDE-209	Br$_{<10}$-PBDEs	ΣBDEs	Reference
Land								
China	Spring and Fall 2008	8	PASs	Gas		15.4 ± 13.8		(Li et al., 2014)
South Korea	Spring and Fall 2008	8	PASs	Gas		7.05 ± 6.36		
Japan	Spring and Fall 2018	8	PASs	Gas		2.47 ± 1.12		
Across China	September 2008 to August 2009	12	PUF	Gas&TSP			232 ± 72	(Yang et al., 2013)
				Gas	nd-77.0			
				TSP	1.06–728			
Guangzhou	September 2008 to August 2009	12	PUF	Gas&TSP			838 ± 126	
Beijing	September 2008 to August 2009	12	PUF	Gas&TSP			781 ± 107	
Dalian	September 2008 to August 2009	12	PUF	Gas&TSP			104 ± 95	(Yang et al., 2012)
E-waste dismantling site (Guiyu)	September 13–21, 2005	11	PUF	Gas&TSP	2164	9579	11,742 (Day)	(Chen et al., 2009)
					1649	3182	4830 (Night)	
Laizhou Bay	2007	11	PUF	Gas			0.017–1.17*	(Jin et al., 2011)
				TSP			0.5–161.1*	
Lake Chaohu	May 2010 to July 2013	14	PUF	Gas&TSP	3.9–262.3 (58.5)	3.5–201 (27.6)		(He et al., 2014)
Taihu Lake	2004	33					220	(Qiu et al., 2010)
Great Lakes region	April to November 2012	7	PEs	Gas		0.1–11		(McDonough et al., 2016)
Shanghai rural regions	June 2012 to May 2013	12	PUF	Gas		8.07–77.5 (Summer) 4.49–35.31 (Winter)		(Zhu et al., 2017)
Alert, Nunavut	October 2006 to February 2008	14	FTS			1.2–55		(Xiao et al., 2012)
Nam Co, Tibet	Weekly since 1992	28	PUF	Gas&TSP			0.83–5.2	(Xiao et al., 2012)
HN Island	October 25,2011 to August 14, 2012	12		PM2.5	7.1 ± 6.8	0.97 ± 0.52		(Li et al. (2015a, 2015b))
HN Island	October 2013 to August 2014	9	PUF	TSP	12.8 ± 23.7	1.2 ± 2.3	14.0 ± 25.5	This study
				Gas	5.4 ± 8.0	0.9 ± 0.7	6.3 ± 8.0	
Ocean								
East and South China Seas	Jan 16 to Mar 14, 2008		PUF/XAD-2	Gas&TSP		10.8 ± 6.13		(Li et al., 2011)
Bay of Bengal and the Andaman Sea	Jan 16 to Mar 14, 2008					3.22 ± 1.57		
Indian Ocean	Jan 16 to Mar 14, 2008					5.12 ± 3.56		
Atlantic Ocean	Jan 16 to Mar 14, 2008					2.87 ± 1.81		
Atlantic and the Southern Ocean	November and December 2008	9	PUF/XAD-2	Gas		0.32–2.85		(Xie et al., 2011)
				TSP		<0.04–2.16		
East China Sea to the high Arctic	June to September 2010	10	PUF/XAD-2	Gas&TSP	nd-4.0		0.07–8.1	(Möller et al., 2012a)
North Sea	2010	6		Gas&TSP			0.31–10.7	(Möller et al., 2012a)
East Greenland Sea	August and September 2009	10	PUF/XAD-2	Gas			0.09–1.8	(Möller et al., 2011b)
				TSP			0.03–0.64	
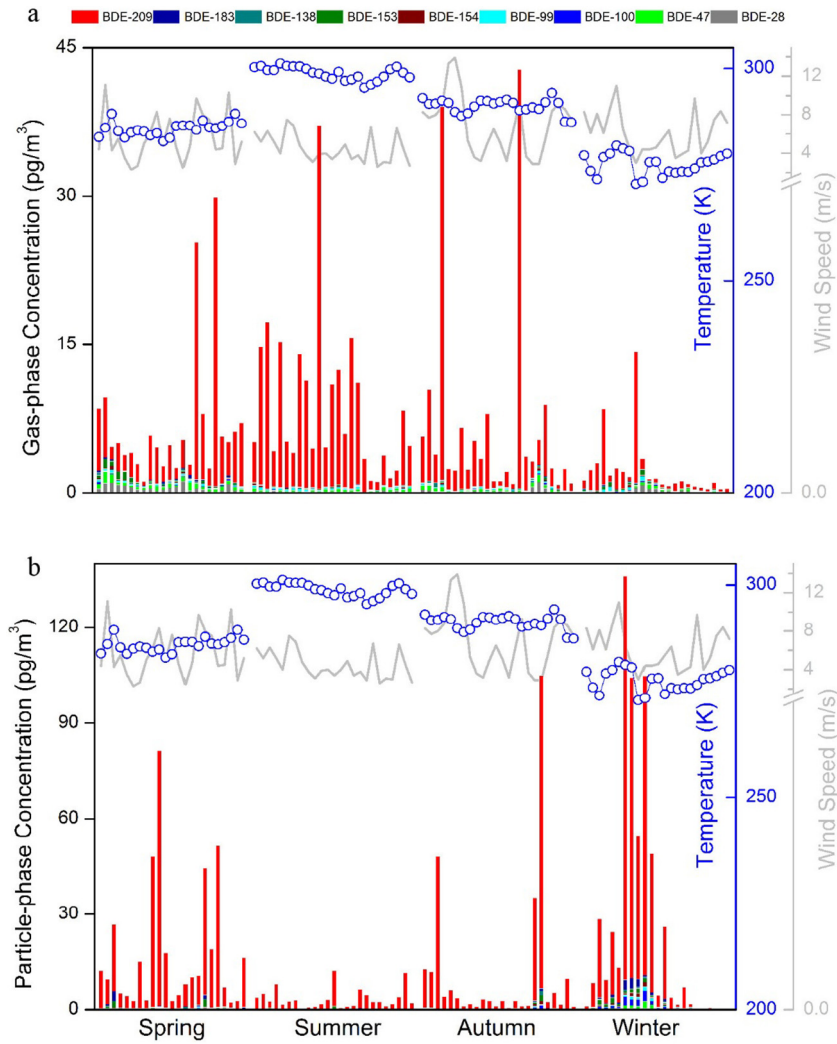
Fig. 2. Concentrations of PBDE congeners in atmospheric samples (gas and particle phases), as well as ambient temperature and wind speed at Huaniao Island, Yangtze River Estuary, in 2013–2014.

Archipelago toward the Indian Ocean and then to the Southern Ocean (Möller et al., 2012b). The PBDE concentrations in our study were in the range of those observed at background and urban sites (Table 1). Because there was almost no industrial activity on the island (Li et al., 2015a), the relative PBDEs level should have been under the influence of continental outflow.

For Br$_{<10}$-BDEs, the legacy flame retardants, the annual average concentrations of Σ_8BDEs were 0.9 ± 0.7 pg/m^3 and 1.2 ± 2.2 pg/m^3 in the gas and particle phases, respectively. Although various sampling methods were applied, the concentrations of Σ_8BDEs over the YRE were similar to those over remote sites and open seas (Table 1), consistent with the limited usage and recent prohibition of penta- and octa-BDE technical products in China. As reported previously, the phasing out of penta-BDE and octa-BDE mixtures in China has helped reduce atmospheric PBDE concentrations in China (Liu et al., 2016).

Among these PBDE congeners, BDE-209 was dominant in both the gas (5.4 ± 8.0 pg/m^3) and particle (12.8 ± 26.7 pg/m^3) phases. This was in good agreement with observations in surrounding areas of the ECS and consistent with the fact that high BDE-209 concentrations have been detected widely in China (Rahman et al., 2001). The China-POPs SAMP-II data showed that concentrations of BDE-209 in the gas phase were in the range of 10.2–77.0 pg/m^3 for urban sites, 8.3 pg/m^3 for suburban sites, and below the detection limit for remote/rural sites, whereas concentrations in the particle phase were in the range of 10.7–728 pg/m^3, 46.4 pg/m^3, and

1.0–6.2 pg/m^3, respectively (Li et al., 2016b). The concentrations of BDE-209 over the YRE were in the range of those detected over suburban and background sites in China (Table 1). High BDE-209 concentrations, with contributions of 86% and 92% to the total PBDEs
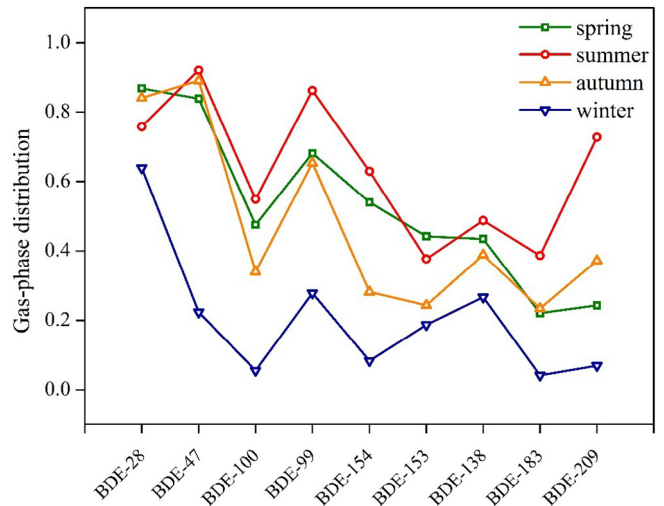

Fig. 3. Relative gas-phase distributions of individual PBDEs over the Yangtze River Estuary.
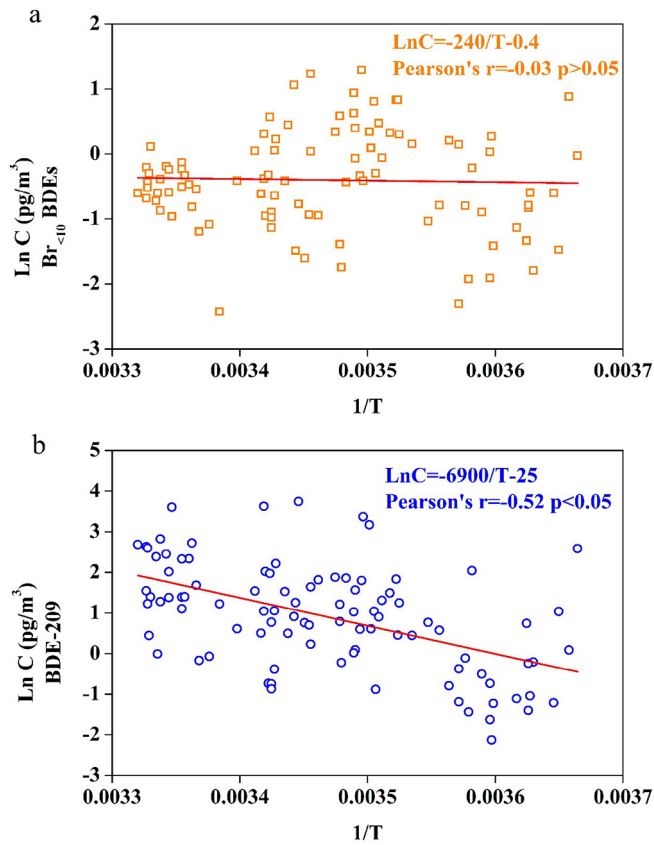
Fig. 4. Correlation analysis between gas-phase concentrations of PBDEs and reciprocal temperature (K).

measured in gas and particle phase, respectively, were observed, consistent with the BDE-209 usage record in China (Li et al., 2016a, 2016b). Therefore, like most areas in China, the YRE region can be

regarded as relatively uncontaminated with Br$_{<10}$-BDEs but more dominantly contaminated with BDE-209.

3.2. Seasonal variation

Seasonal variation of particle phase PBDEs was observed, with the highest concentration in winter (25.2 pg/m^3) and the lowest in summer (3.3 pg/m^3), as shown in Fig. 2. As shown by the backward trajectory in Fig. S1, northwesterly and northerly winds were dominant in winter, carrying atmospheric pollutants from North China. In other seasons, the wind direction varied and often transported cleaner air masses from the ocean. In addition, good correlations were found among all particle-phase PBDE congeners, with Pearson's r ranging from 0.33 to 0.95 ($p < 0.05$), suggesting that these congeners could be emitted from a common source or could exhibit a common environmental behavior, e.g., long-range transport over land. These results indicated that atmospheric transport was an important influencing factor of particle-phase PBDE concentrations in the YRE region.

In the gas phase, total PBDEs showed the inverse seasonal trend, with the highest concentration in summer (8.8 pg/m^3) and the lowest in winter (2.3 pg/m^3). A similar seasonal variation was observed for gas-phase BDE-209, where summer (8.2 pg/m^3) > autumn (6.1 pg/m^3) > spring (5.3 pg/m^3) > winter (1.7 pg/m^3). However, Br$_{<10}$-BDEs showed no significant seasonal trend, although concentrations were higher in spring.

The seasonal gas-phase concentration variations seemed to be significantly associated with the phase distribution of PBDEs in different seasons. For instance, low-brominated BDE congeners were prone to distribution mainly in the gas phase due to their higher vapor pressure values (Fig. 3). Low-brominated PBDEs may occur in the atmosphere as secondary emissions via the air–surface exchange process. However, high-brominated BDEs were mainly associated with the particle phase, particularly in the cold season. Notably, the distribution of all BDE congeners, except for BDE-28, shifted to being particle-phase dominant in winter, possibly due to temperature-influenced phase distribution. Thus, to assess the influence of the temperature-influenced phase distribution of PBDEs, correlation analysis between the logarithms of
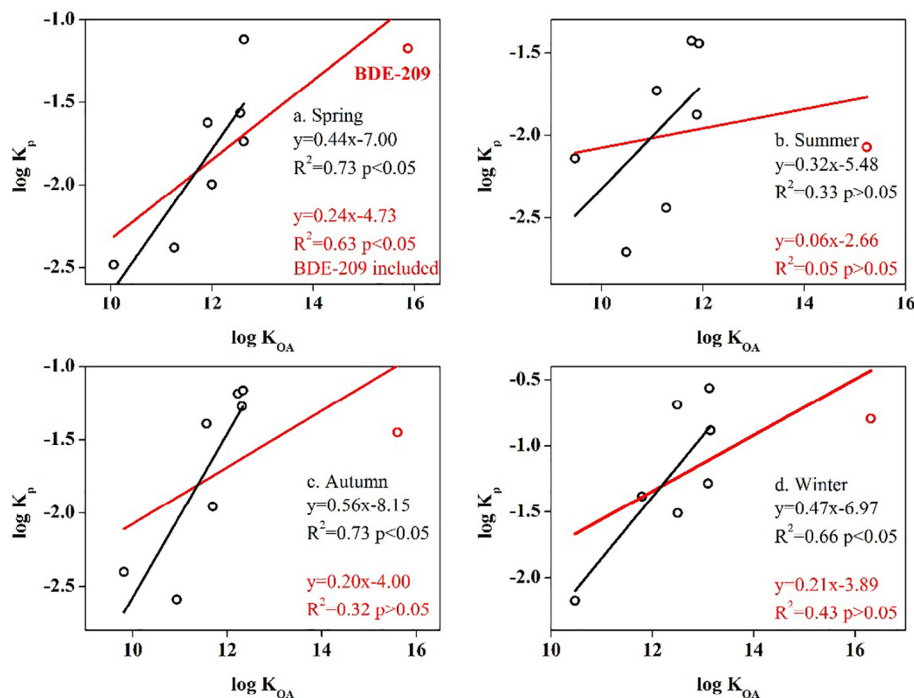

Fig. 5. Correlations between log Kp and log KOA in samples during the four seasons. Red represents BDE-209. (For interpretation of the references to colour in this figure legend, the reader is referred to the web version of this article.)

gas-phase PBDE congener concentrations and reciprocal temperature ($1/T$) was performed (Fig. 4). Ambient temperature is considered to be an important control of the seasonality of SVOCs in air due to its marked effect on the chemical partitioning between air and surface media (e.g., soil and water) (Cousins et al., 1999; Nizzetto et al., 2010). The logarithms of gas-phase concentrations of SVOCs should generally be well regressed with reciprocal temperature (Wania et al., 1998). However, in our study, no significant correlation was found between the logarithm of gas-phase Br$_{<10}$-BDE concentrations and reciprocal temperature (Pearson's $r = -0.32$, $p > 0.05$), possibly corresponding to their low residual level in the environment, while a weak correlation was observed between the logarithms of gas-phase BDE-209 concentrations and reciprocal temperature (Pearson's $r = -0.52$, $p < 0.05$). That is, other parameters aside from ambient temperature likely affect the phase distribution of PBDEs, which is possibly influenced by the seasonal variation of sources.

3.3. Gas–particle partition

HNI is in the atmospheric pathway of continental outflow, and is influenced by the prevailing winds of the East Asian Monsoon. The fate, transport, and removal of PBDEs from the atmosphere are strongly influenced by gas–particle partitioning (Lohmann et al., 2000). In addition, the equilibrium or non-equilibrium condition of the gas–particle partitioning could provide information about the occurrence of inputs of atmospheric PBDEs.

3.3.1. Comparison between P_L^0 and K_p

The relationship between the logarithms of the seasonal mean K_p and P_L^0 of the BDE compounds (excluding BDE-138 and -209 due to data unavailability) was calculated. The values of P_L^0 were temperature dependent and calculated from the equation reported by Tittlemier et al. (2002). Good correlation between the logarithms of seasonal mean K_p and P_L^0 was found for spring and autumn atmospheric samples ($R^2 > 0.76$, $p < 0.01$) (Fig. S2). Moderate correlation was observed for summer ($R^2 = 0.45$, $p > 0.05$) and winter ($R^2 = 0.62$, $p < 0.05$) samples, along with shallower slopes (m_p, -0.27 and -0.30, respectively). The slope of the regression plots derived from the air sampling data deviated largely from -1, possibly because of sampling artifacts, non-equilibrium conditions, varying activity coefficients in organic matter in a compound class, or thermodynamic factors (Cetin and Odabasi, 2008; Yang et al., 2013). Experimental field data on gas–particle partitioning often may not represent the true partitioning equilibrium (Pankow and Bidleman, 1992). The regression slope in our study in summer and winter was within the range of values reported for urban and background sites (Chen et al., 2006; Cetin and Odabasi, 2008; Besis et al., 2016) and close to the whole-year observation in a northeastern urban city in China (-0.3) (Yang et al., 2012). The m_r values derived from log–log plots of K_p versus P_L^0 can provide insights into the mechanisms governing gas–particle partitioning. The slope values from log–log plots of K_p versus P_L^0 can be used to classify the type of sorption process: $m_p < -1$, surface adsorption; $m_p > -0.6$, absorption by organic matter; and $-1 < m_p < -0.6$, coexistence of both mechanisms (Goss and Schwarzenbach, 1998). The values of m_p in this study exceeded -0.6, suggesting that absorption was the dominant mechanism.

3.3.2. Comparison between K_{OA} and K_p

K_{OA} was used to describe gas–particle partitioning, with the assumption that absorption was the dominant process of the SVOCs (Harner and Bidleman, 1998; Harner and Shoeib, 2002; Cetin and Odabasi, 2008). The K_{OA} values of the PBDEs were calculated using reported temperature-dependent K_{OA} values, excluding BDE-138 (data unavailable) (Harner and Shoeib, 2002; Li et al., 2016a, 2016b).

Like the slope m_p, the slope m_o between log K_p and log K_{OA} commonly deviates from 1 (i.e., equilibrium state) in field observations;

such deviations were also observed in the present study. Generally, the correlation between log K_p and log K_{OA} is used to indicate the equilibrium state of gas–particle partitioning of PBDEs. There was an obviously seasonal variation in the correlation between log K_p and log K_{OA}, as shown in Fig. 5. Good correlation was found for Br$_{<10}$-BDEs in spring
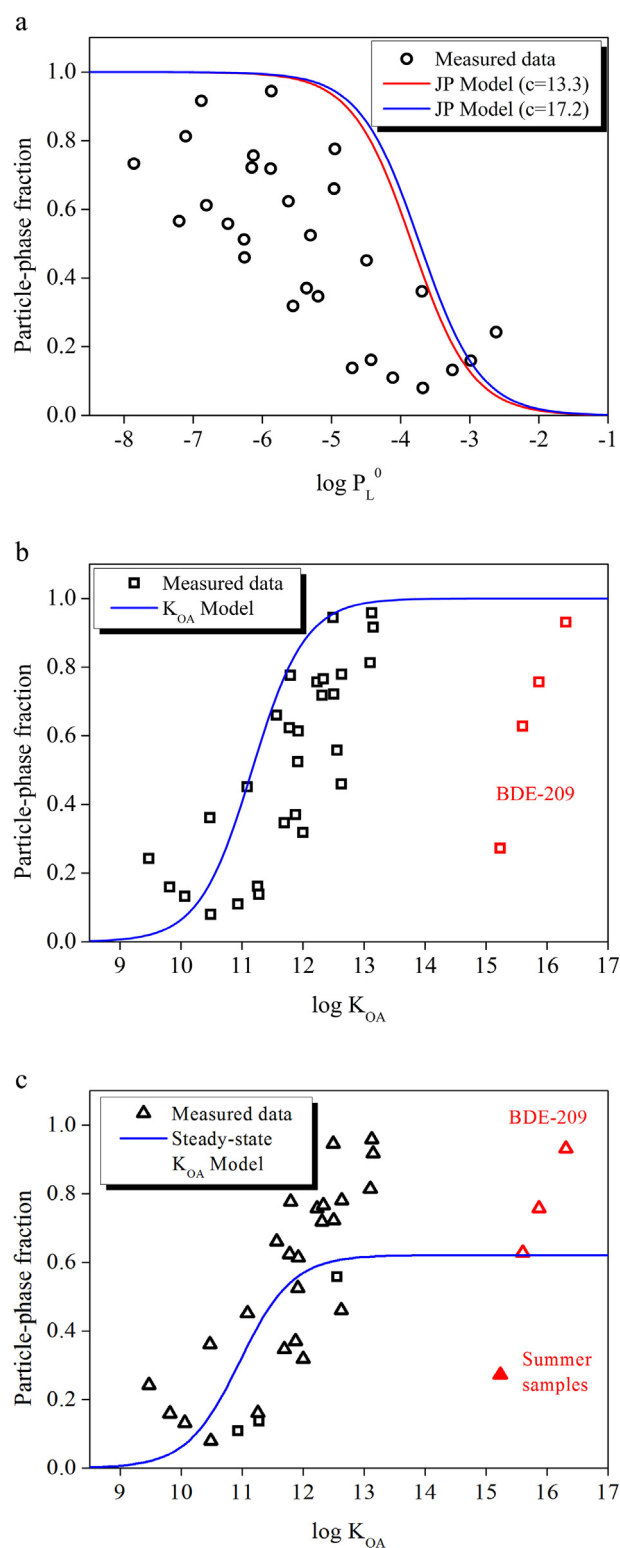

Fig. 6. Comparison of the measured particulate fractions of PBDEs (Φ) with the Junge–Pankow adsorption model ($c = 17.2$ and 13.3 Pa cm), the K_{OA}-based absorption model and a steady-state absorption model ($C = 5$ and $G = 2.09 \times 10^{-10}$ f_{om} K_{OA}) (Li et al., 2016a, 2016b; Besis et al., 2017).

and autumn ($R^2 = 0.73$ and 0.73, respectively, $p < 0.05$). Moderate correlation was found in winter ($R^2 = 0.66$, $p < 0.05$), whereas relatively weak correlation occurred in summer ($R^2 = 0.33$, $p > 0.05$). These were similar to the correlation results between log K_p and log P_L^o, indicating that the aerosol organic matter has sorption properties differed from the case in the model solvent octanol or that phase equilibrium was not established, especially in summer (Goss and Schwarzenbach, 1998).

Furthermore, when BDE-209 was included in the correlation analysis between log K_p and log K_{OA}, the correlation got worsen in all four seasons, and the slopes became shallower. One possible reason is the slow re-equilibration process between reemitted POPs in the environment and freshly emitted particulate matter in the atmosphere (Lohmann et al., 2000). In particular, higher-molecular-weight species attain equilibrium more slowly than low-molecular-weight compounds (Kamens et al., 1995; Simcik et al., 1998). Second, continuous gas-phase
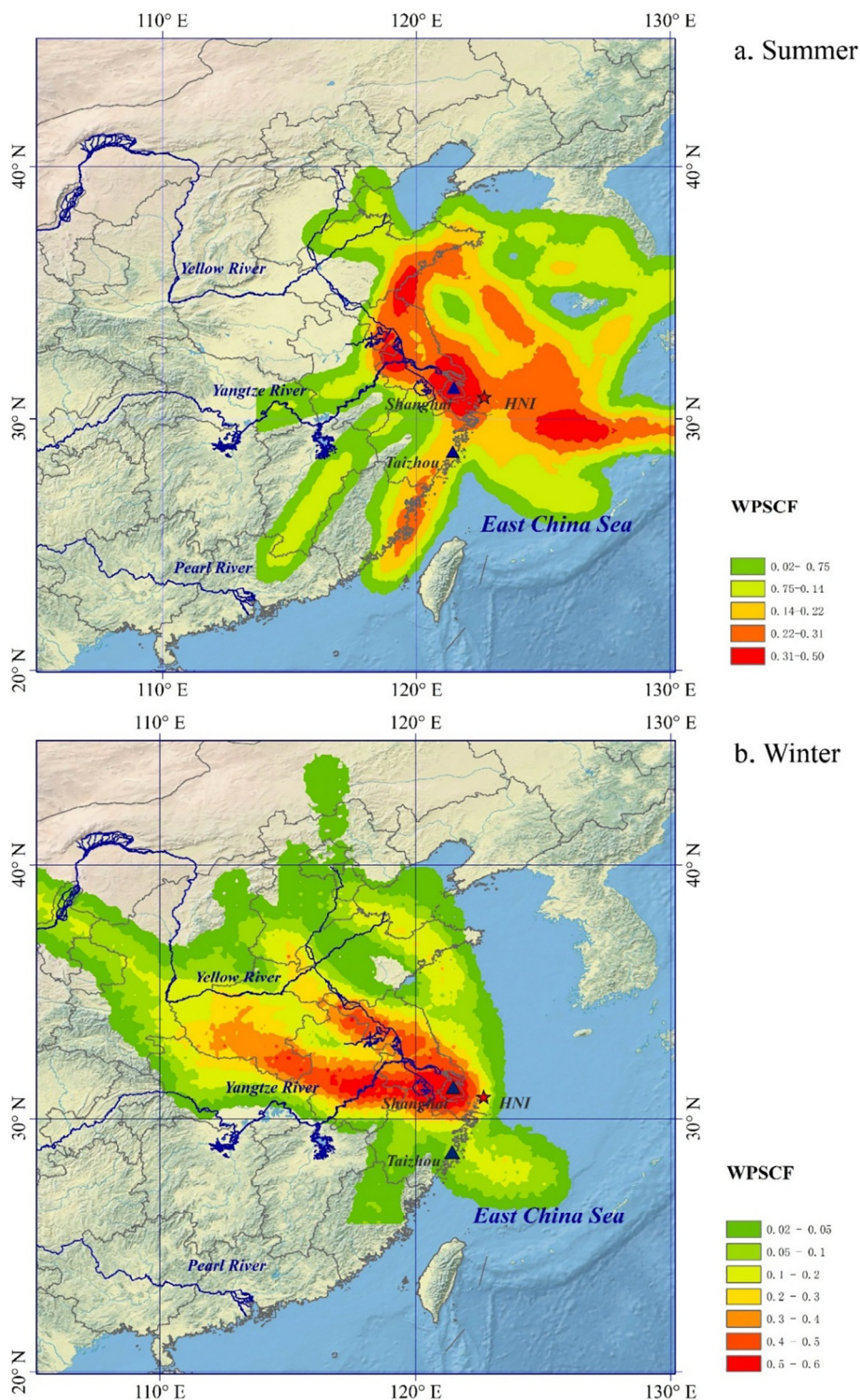

Fig. 7. Potential source regions of BDE-209 based on summer and winter samples collected in 2013–2014 over the Yangtze River Estuary.

pollutant emissions should be expected in the ambient environment. This speculation was further evidenced by the gas-phase distribution of BDE-209. Generally, the gas-phase distribution of individual BDE congeners decreased markedly with increasing bromine substitution (Fig. 3). An exception was observed for BDE-209, with a relatively higher gas-phase distribution than other high-brominated BDEs (BDE-153, −154, −138, and −183). The gas-phase distribution reached 73% in summer. A similar phase distribution was reported by Agrell et al. (2004), who found that BDE-209 was mainly in the gas phase (> 90%) at an urban site, and almost entirely in the gas phase at a rural site, possibly due to adjacency to nearby emissions. These results could indicate the input of gas-phase BDE-209 in the study area, i.e., due to volatilization or gas-phase transmission from land emission in summer (see Section 3.4).

3.3.3. Model prediction

The particle-phase fraction Φ of SVOCs can be predicted conventionally by the Junge–Pankow adsorption (P_L^0-based) model, the K_{OA}-based absorption model as well as a steady-state absorption model including an equilibrium and a non-equilibrium term (Cincinelli et al., 2014; Besis et al., 2016; Li et al., 2015a, 2016b). The details of these three models are described in the Supplementary Material. The K_{OA}-based model appeared to predict the measured Φ relatively better than the Junge–Pankow adsorption model, especially for Br$_{<10}$-BDEs, highlighting the absorptive role of the organic content of particles (Fig. 6) (Samara et al., 2014; Besis et al., 2015). However, the K_{OA}-based adsorption model seemed to largely overestimate the particle-phase fraction of BDE-209. While the steady-state model proved to be superior to predict G/P partitioning of BDE-209 based on annual values (Li et al., 2016b; Besis et al., 2017), though with the exception of summer samples. The overestimation of the particle-phase fraction of BDE-209, consistent with the above correlation analysis, indicated the input of gas-phase BDE-209, especially during warmer seasons.

3.4. Potential sources of BDE-209 from atmospheric long-range transport

The PSCF was used to identify the possible source regions for atmospheric BDE-209 in different seasons. The YRE is located in the atmospheric route of continental outflow triggered by the prevailing winds of the East Asian Monsoon. The densely populated northern and eastern areas of China, especially the YRD region, were clear high-pollution source regions of particle-phase BDE-209 in winter (Fig. 7b). Under the driving force of the prevailing northwesterly and northerly winds, winter air masses passed through the aforementioned source regions of PBDEs, leading to relatively high abundances of BDE-209 in the downwind YRE area.

In summer, due to variations in wind direction, the potential source regions of atmospheric BDE-209 were more diverse (Fig. 7a) and mainly included Shandong and Jiangsu Provinces, the YRD region, and the southeastern coastal areas with intensive e-waste recycling activities (e.g., Taizhou in Zhejiang Province). As discussed above, PBDE re-emission from various environmental matrices potentially enhanced the atmospheric burden in summer (Gevao et al., 2013; Besis et al., 2015; Xu et al., 2015a, 2015b). Domestic deca-BDE manufacturing facilities are primarily located in the Shandong Peninsula and Jiangsu Province (Zhang and Lu, 2011); for example, Σ_{11}PBDEs reached levels as high as 0.4 and 40 ng/m^3 in the gas and particle phases in Laizhou Bay in summer, respectively (Jin et al., 2011). In addition, the YRD region and southeastern coastal areas, which are characterized by intensive industrial activities and urban development, are host to thousands of rapidly growing factories, including those for textiles, furniture, electrical and electronic devices, and toys, which can contain PBDEs (Li et al., 2012). For instance, gas- and particle-phase BDE-209 concentrations reached 800–1200 pg/m^3 in three cities (Suzhou, Wuxi and Nantong) in the Yangtze River Delta (Zhang et al., 2013). More importantly, the coast of Taizhou (Zhejiang Province) has become a growing center for e-waste recycling and receives both domestic and foreign e-wastes (Li et al., 2016a, 2016b). High concentrations of PBDEs have been found in the air and soil of typical e-waste dismantling areas in Taizhou (Yu et al., 2016). Zhang et al. (2012) reported increased atmospheric concentrations of more highly brominated PBDEs in summer (average: 165 pg/m^3) over Taizhou, and Han et al. (2009) reported that BDE-209 was a major component of all collected atmospheric samples (70%) over Taizhou. Thus, it can be inferred from Fig. 7 that gas-phase BDE-209 would be volatilized and transported along with the air masses under the high-temperature conditions during summer, causing relatively high gas-phase BDE-209 levels over coastal regions of the ECS, as well as further east.

4. Conclusion

This work reported, for the first time, the annual occurrence of both gas- and particle-phase PBDEs over the YRE and analyzed their gas–particle partitioning. Among PBDE congeners, BDE-209 was dominant in both the gas and particle phases, consistent with the BDE-209 usage record in China. Comparisons between both K_{OA} and P_L^0 with K_p indicated that the gas–particle partitioning of PBDEs was in a non-equilibrium state. The slope m_p as well as m_o was generally deviated from the equilibrium state in filed observations, including our study. Instead, we use the correlation between log K_p and log K_{OA} to indicate the equilibrium state of gas-particle partitioning of PBDEs. The correlation between K_{OA} and K_p worsened and the slopes became shallower when BDE-209 was included in above correlation analysis, possibly due to fresh emissions of gas-phase BDE-209, especially in summer. In addition, the K_{OA}-based adsorption model prediction greatly overestimated the particle-phase fraction of BDE-209. The steady-state model reproduced well for G/P partitioning of BDE-209 based on annual values; but large prediction still existed in summer samples. Together, these combined results emphasize the significance of atmospheric transport of BDE-209 from land emissions in both phases, which may originate from various highly BDE-contaminated regions. For these SVOCs, additional observations of both gas- and particle-phase pollution level should be conducted in source regions, given the importance of gas-phase transport.

Acknowledgement

Appendix A. Supplementary material

Supplementary material to this article can be found online at https://doi.org/10.1016/j.scitotenv.2019.07.344.

References

Agrell, C., ter Schure, A.F., Sveder, J., Bokenstrand, A., Larsson, P., Zegers, B.N., 2004. Polybrominated diphenyl ethers (PBDES) at a solid waste incineration plant I: atmospheric concentrations. Atmos. Environ. 38 (30), 5139–5148.

Ashbaugh, L.L., Malm, W.C., Sadeh, W.Z., 1985. A residence time probability analysis of sulfur concentrations at Grand Canyon National Park. Atmos. Environ. (1967) 19 (8), 1263–1270.

Bergman, Å., Rydén, A., Law, R.J., de Boer, J., Covaci, A., Alaee, M., Birnbaum, L., Petreas, M., Rose, M., Sakai, S., Van den Eede, N., van der Veen, I., 2012. A novel abbreviation standard for organobromine, organochlorine and organophosphorus flame retardants and some characteristics of the chemicals. Environ. Int. 49, 57–82.

Besis, A., Botsaropoulou, E., Voutsa, D., Samara, C., 2015. Particle-size distribution of polybrominated diphenyl ethers (PBDEs) in the urban agglomeration of Thessaloniki, northern Greece. Atmos. Environ. 104, 176–185.

Besis, A., Voutsa, D., Samara, C., 2016. Atmospheric occurrence and gas-particle partitioning of PBDEs at industrial, urban and suburban sites of Thessaloniki, northern Greece: implications for human health. Environ. Pollut. 215, 113–124.

Besis, A., Lammel, G., Kukučka, P., Samara, C., Sofuoglu, A., Dumanoglu, Y., Eleftheriadis, K., Kouvarakis, G., Sofuoglu, S.C., Vassilatou, V., 2017. Polybrominated diphenyl ethers (PBDEs) in background air around the Aegean: implications for phase partitioning and size distribution. Environ. Sci. Pollut. R. 24 (36), 28102–28120.

Bi, X., Thomas, G.O., Jones, K.C., Qu, W., Sheng, G., Martin, F.L., Fu, J., 2007. Exposure of electronics dismantling workers to polybrominated diphenyl ethers, polychlorinated biphenyls, and organochlorine pesticides in south China. Environ. Sci. Technol. 41 (16), 5647–5653.

Cetin, B., Odabasi, M., 2008. Atmospheric concentrations and phase partitioning of polybrominated diphenyl ethers (PBDEs) in Izmir, Turkey. Chemosphere 71 (6), 1067–1078.

Chen, L., Mai, B., Bi, X., Chen, S., Wang, X., Ran, Y., Luo, X., Sheng, G., Fu, J., Zeng, E.Y., 2006. Concentration levels, compositional profiles, and gas-particle partitioning of polybrominated diphenyl ethers in the atmosphere of an urban city in south China. Environ. Sci. Technol. 40 (4), 1190–1196.

Chen, D., Bi, X., Zhao, J., Chen, L., Tan, J., Mai, B., Sheng, G., Fu, J., Wong, M., 2009. Pollution characterization and diurnal variation of PBDEs in the atmosphere of an E-waste dismantling region. Environ. Pollut. 157 (3), 1051–1057.

Cincinelli, A., Pieri, F., Martellini, T., Passaponti, M., Bubba, M.D., Vento, S.D., Katsoyiannis, A.A., 2014. Atmospheric occurrence and gas-particle partitioning of PBDEs in an industrialised and urban area of Florence, Italy. Aerosol Air Qual. Res. 14 (4), 1121–1130.

Cousins, I.T., Beck, A.J., Jones, K.C., 1999. A review of the processes involved in the exchange of semi-volatile organic compounds (SVOC) across the air–soil interface. Sci. Total Environ. 228 (1), 5–24.

Darnerud, P.O., Eriksen, G.S., Johannesson, T., Larsen, P.B., Viluksela, M., 2001. Polybrominated diphenyl ethers: occurrence, dietary exposure, and toxicology. Environ. Health Perspect. 109 (Suppl. 1), 49–68.

Finizio, A., Mackay, D., Bidleman, T., Harner, T., 1997. Octanol-air partition coefficient as a predictor of partitioning of semi-volatile organic chemicals to aerosols. Atmos. Environ. 31 (15), 2289–2296.

Gevao, B., Ghadban, A.N., Porcelli, M., Ali, L., Rashdan, A., Al-Bahloul, M., Matrouk, K., Zafar, J., 2013. Seasonal variations in the atmospheric concentrations of polybrominated diphenyl ethers in Kuwait. Sci. Total Environ. 454-455, 534–541.

Goss, K., Schwarzenbach, R.P., 1998. Gas/solid and gas/liquid partitioning of organic compounds: critical evaluation of the interpretation of equilibrium constants. Environ. Sci. Technol. 32 (14), 2025–2032.

Han, W., Feng, J., Gu, Z., Chen, D., Wu, M., Fu, J., 2009. Polybrominated diphenyl ethers in the atmosphere of Taizhou, a major E-waste dismantling area in China. B. Environ. Contam. Tox. 83 (6), 783–788.

Harner, T., Bidleman, T.F., 1998. Octanol— air partition coefficient for describing particle/gas partitioning of aromatic compounds in urban air. Environ. Sci. Technol. 32 (10), 1494–1502.

Harner, T., Shoeib, M., 2002. Measurements of octanol—air partition coefficients (K_{OA}) for polybrominated diphenyl ethers (PBDEs): predicting partitioning in the environment. J. Chem. Eng. Data 47 (2), 228–232.

He, W., Qin, N., He, Q., Kong, X., Liu, W., Wang, Q., Yang, C., Jiang, Y., Yang, B., Bai, Z., Wu, W., Xu, F., 2014. Atmospheric PBDEs at rural and urban sites in central China from 2010 to 2013: residual levels, potential sources and human exposure. Environ. Pollut. 192, 232–243.

Hsu, Y., Holsen, T.M., Hopke, P.K., 2003. Locating and quantifying PCB sources in Chicago: receptor modeling and field sampling. Environ. Sci. Technol. 37 (4), 681–690.

Ji, X., Ding, J., Xie, X., Cheng, Y., Huang, Y., Qin, L., Han, C., 2017. Pollution status and human exposure of decabromodiphenyl ether (BDE-209) in China. ACS Omega 2 (7), 3333–3348.

Jiang, Y., Lin, T., Wu, Z., Li, Y., Li, Z., Guo, Z., Yao, X., 2018. Seasonal atmospheric deposition and air–sea gas exchange of polycyclic aromatic hydrocarbons over the Yangtze River Estuary, East China Sea: implications for source–sink processes. Atmos. Environ. 178, 31–40.

Jin, J., Wang, Y., Liu, W., Yang, C., Hu, J., Cui, J., 2011. Polybrominated diphenyl ethers in atmosphere and soil of a production area in China: levels and partitioning. J. Environ. Sci.-China 23 (3), 427–433.

Kamens, R., Odum, J., Fan, Z., 1995. Some observations on times to equilibrium for semivolatile polycyclic aromatic hydrocarbons. Environ. Sci. Technol. 29 (1), 43–50.

Li, J., Li, Q., Gioia, R., Zhang, Y., Zhang, G., Li, X., Spiro, B., Bhatia, R.S., Jones, K.C., 2011. PBDEs in the atmosphere over the Asian marginal seas, and the Indian and Atlantic oceans. Atmos. Environ. 45 (37), 6622–6628.

Li, Y., Lin, T., Chen, Y., Hu, L., Guo, Z., Zhang, G., 2012. Polybrominated diphenyl ethers (PBDEs) in sediments of the coastal East China Sea: occurrence, distribution and mass inventory. Environ. Pollut. 171, 155–161.

Li, Q., Li, J., Chaemfa, C., Zhang, G., Kobara, Y., Nam, J., Jones, K.C., 2014. The impact of polybrominated diphenyl ether prohibition: a case study on the atmospheric levels in China, Japan and South Korea. Atmos. Res. 143, 57–63.

Li, Y., Lin, T., Wang, F., Ji, T., Guo, Z., 2015a. Seasonal variation of polybrominated diphenyl ethers in PM2.5 aerosols over the East China Sea. Chemosphere 119, 675–681.

Li, Y.F., Ma, W.L., Yang, M., 2015b. Prediction of gas/particle partitioning of polybrominated diphenyl ethers (PBDEs) in global air: a theoretical study. Atmos. Chem. Phys. 15 (4), 1669–1681.

Li, Y., Lin, T., Hu, L., Feng, J., Guo, Z., 2016a. Time trends of polybrominated diphenyl ethers in East China Seas: response to the booming of PBDE pollution industry in China. Environ. Int. 92-93, 507–514.

Li, Y., Qiao, L., Ren, N., Sverko, E., Mackay, D., Macdonald, R.W., 2016b. Decabrominated diphenyl ethers (BDE-209) in Chinese and global air: levels, gas/particle partitioning, and long-range transport: is long-range transport of BDE-209 really governed by the movement of particles? Environ. Sci. Technol. 51 (2), 1035–1042.

Li, Z., Lin, T., Li, Y., Jiang, Y., Guo, Z., 2017. Atmospheric deposition and air-sea gas exchange fluxes of DDT and HCH in the Yangtze River Estuary, East China Sea. J. Geophys. Res.-Atmos. 122 (14), 7664–7677.

Liu, L., Ma, W., Jia, H., Zhang, Z., Song, W., Li, Y., 2016. Research on persistent organic pollutants in China on a national scale: 10 years after the enforcement of the Stockholm convention. Environ. Pollut. 217, 70–81.

Lohmann, R., Harner, T., Thomas, G.O., Jones, K.C., 2000. A comparative study of the gas-particle partitioning of PCDD/Fs, PCBs, and PAHs. Environ. Sci. Technol. 34 (23), 4943–4951.

Ma, J., Qiu, X., Zhang, J., Duan, X., Zhu, T., 2012. State of polybrominated diphenyl ethers in China: an overview. Chemosphere 88 (7), 769–778.

McDonough, C.A., Puggioni, G., Helm, P.A., Muir, D., Lohmann, R., 2016. Spatial distribution and air–water exchange of organic flame retardants in the Lower Great Lakes. Environ. Sci. Technol. 50 (17), 9133–9141.

Möller, A., Xie, Z., Cai, M., Zhong, G., Huang, P., Cai, M., Sturm, R., He, J., Ebinghaus, R., 2011a. Polybrominated diphenyl ethers vs alternate brominated flame retardants and dechloranes from East Asia to the Arctic. Environ. Sci. Technol. 45 (16), 6793–6799.

Möller, A., Xie, Z., Sturm, R., Ebinghaus, R., 2011b. Polybrominated diphenyl ethers (PBDEs) and alternative brominated flame retardants in air and seawater of the European Arctic. Environ. Pollut. 159 (6), 1577–1583.

Möller, A., Xie, Z., Caba, A., Sturm, R., Ebinghaus, R., 2012a. Occurrence and air-seawater exchange of brominated flame retardants and Dechlorane Plus in the North Sea. Atmos. Environ. 46, 346–353.

Möller, A., Xie, Z., Cai, M., Sturm, R., Ebinghaus, R., 2012b. Brominated flame retardants and Dechlorane plus in the marine atmosphere from Southeast Asia toward Antarctica. Environ. Sci. Technol. 46 (6), 3141–3148.

Ni, K., Lu, Y., Wang, T., Shi, Y., Kannan, K., Xu, L., Li, Q., Liu, S., 2013. Polybrominated diphenyl ethers (PBDEs) in China: policies and recommendations for sound management of plastics from electronic wastes. J. Environ. Manag. 115, 114–123.

Nizzetto, L., Macleod, M., Borgå, K., Cabrerizo, A., Dachs, J., Guardo, A.D., Ghirardello, D., Hansen, K.M., Jarvis, A., Lindroth, A., Ludwig, B., Monteith, D., Perlinger, J.A., Scheringer, M., Schwendenmann, L., Semple, K.T., Wick, L.Y., Zhang, G., Jones, K.C., 2010. Past, present, and future controls on levels of persistent organic pollutants in the global environment. Environ. Sci. Technol. 44 (17), 6526–6531.

Pankow, J.F., 1994. An absorption model of gas/particle partitioning of organic compounds in the atmosphere. Atmos. Environ. 28 (2), 185–188.

Pankow, J.F., Bidleman, T.F., 1992. Interdependence of the slopes and intercepts from log-log correlations of measured gas-particle partitioning and vapor pressure—I. theory and analysis of available data. Atmos. Environ. Part A 26 (6), 1071–1080.

Qiu, X., Zhu, T., Hu, J., 2010. Polybrominated diphenyl ethers (PBDEs) and other flame retardants in the atmosphere and water from Taihu Lake, East China. Chemosphere 80 (10), 1207–1212.

Rahman, F., Langford, K.H., Scrimshaw, M.D., Lester, J.N., 2001. Polybrominated diphenyl ether (PBDE) flame retardants. Sci. Total Environ. 275 (1–3), 1–17.

Samara, C., Voutsa, D., Kouras, A., Eleftheriadis, K., Maggos, T., Saraga, D., Petrakakis, M., 2014. Organic and elemental carbon associated to PM10 and PM2.5 at urban sites of northern Greece. Environ. Sci. Pollut. R. 21 (3), 1769–1785.

Simcik, M.F., Franz, T.P., Zhang, H., Eisenreich, S.J., 1998. Gas-particle partitioning of PCBs and PAHs in the Chicago urban and adjacent coastal atmosphere: states of equilibrium. Environ. Sci. Technol. 32 (2), 251–257.

Tian, M., Chen, S., Wang, J., Zheng, X., Luo, X., Mai, B., 2011. Brominated flame retardants in the atmosphere of E-waste and rural sites in southern China: seasonal variation, temperature dependence, and gas-particle partitioning. Environ. Sci. Technol. 45 (20), 8819–8825.

Tittlemier, S.A., Halldorson, T., Stern, G.A., Tomy, G.T., 2002. Vapor pressures, aqueous solubilities, and Henry's law constants of some brominated flame retardants. Environ. Toxicol. Chem. 21 (9), 1804–1810.

Venier, M., Hites, R.A., 2008. Flame retardants in the atmosphere near the Great Lakes. Environ. Sci. Technol. 42 (13), 4745–4751.

Wang, X., Gong, P., Yao, T., Jones, K.C., 2010. Passive air sampling of organochlorine pesticides, polychlorinated biphenyls, and polybrominated diphenyl ethers across the Tibetan plateau. Environ. Sci. Technol. 44 (8), 2988–2993.

Wang, F., Guo, Z., Lin, T., Hu, L., Chen, Y., Zhu, Y., 2015. Characterization of carbonaceous aerosols over the East China Sea: the impact of the East Asian continental outflow. Atmos. Environ. 110, 163–173.

Wang, F., Chen, Y., Meng, X., Fu, J., Wang, B., 2016. The contribution of anthropogenic sources to the aerosols over East China Sea. Atmos. Environ. 127, 22–33.

Wania, F., Haugen, J.E., Lei, Y.D., Mackay, D., 1998. Temperature dependence of atmospheric concentrations of semivolatile organic compounds. Environ. Sci. Technol. 32 (8), 1013–1021.

Xiao, H., Shen, L., Su, Y., Barresi, E., DeJong, M., Hung, H., Lei, Y., Wania, F., Reiner, E.J., Sverko, E., Kang, S., 2012. Atmospheric concentrations of halogenated flame retardants at two remote locations: the Canadian High Arctic and the Tibetan plateau. Environ. Pollut. 161, 154–161.

Xie, Z., Möller, A., Ahrens, L., Sturm, R., Ebinghaus, R., 2011. Brominated flame retardants in seawater and atmosphere of the Atlantic and the Southern Ocean. Environ. Sci. Technol. 45 (5), 1820–1826.

Xu, P., Lou, X., Ding, G., Shen, H., Wu, L., Chen, Z., Han, J., Wang, X., 2015a. Effects of PCBs and PBDEs on thyroid hormone, lymphocyte proliferation, hematology and kidney injury markers in residents of an e-waste dismantling area in Zhejiang, China. Sci. Total Environ. 536, 215–222.

Xu, F., Zhang, G., Wang, J., Zhang, W., Liu, L., Lin, K., 2015b. Polybrominated diphenyl ethers in air and fallouts from an e-waste polluted region in southeast China: insight into levels, compositional profiles, and seasonal variation. Environ. Sci. Pollut. Res. 22 (24), 19676–19686.

Yang, M., Jia, H., Ma, W., Qi, H., Cui, S., Li, Y., 2012. Levels, compositions, and gas-particle partitioning of polybrominated diphenyl ethers and dechlorane plus in air in a Chinese northeastern city. Atmos. Environ. 55, 73–79.

Yang, M., Qi, H., Jia, H., Ren, N., Ding, Y., Ma, W., Liu, L., Hung, H., Sverko, E., Li, Y., 2013. Polybrominated diphenyl ethers in air across China: levels, compositions, and gas-particle partitioning. Environ. Sci. Technol. 47 (15), 8978–8984.

Yu, G., Bu, Q., Cao, Z., Du, X., Xia, J., Wu, M., Huang, J., 2016. Brominated flame retardants (BFRs): a review on environmental contamination in China. Chemosphere 150, 479–490.

Zhang, X., Lu, Q., 2011. Production status and developing prospects of flame retardants. China Plastics Industry 4, 2.

Zhang, T., Huang, Y., Chen, S., Liu, A., Xu, P., Li, N., Qi, L., Ren, Y., Zhou, Z., Mai, B., 2012. PCDD/Fs, PBDD/Fs, and PBDEs in the air of an e-waste recycling area (Taizhou) in China: current levels, composition profiles, and potential cancer risks. J. Environ. Monit. 14 (12), 3156–3163.

Zhang, L., Zhang, T., Dong, L., Shi, S., Zhou, L., Huang, Y., 2013. Assessment of halogenated POPs and PAHs in three cities in the Yangtze River Delta using high-volume samplers. Sci. Total Environ. 454-455, 619–626.

Zhu, Y., Sun, D., Yang, N., Ding, Y., Feng, W., Hong, W., Zhu, S., Li, Y., 2017. Temporal and spatial distributions of PBDEs in atmosphere at Shanghai rural regions, China. Environ. Sci. Pollut. Res. 24 (11), 10885–10892.